Paper AAS 02-109

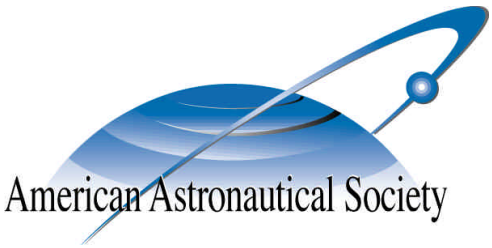

The generalized Sundman transformation for propagation of high-eccentricity elliptical orbits

Matthew Berry and Liam Healy

Naval Research Laboratory

AAS/AIAA Space Flight Mechanics Meeting

San Antonio, Texas **27-30 January, 2002**

AAS Publications Office, P.O. Box 28130, San Diego, CA 92129

AAS 02-109

THE GENERALIZED SUNDMAN TRANSFORMATION FOR PROPAGATION OF HIGH-ECCENTRICITY ELLIPTICAL ORBITS

Matthew Berry* **Liam Healy†**

Abstract

A generalized Sundman transformation $dt = cr^n ds$ for exponent $n \geq 1$ may be used to accelerate the numerical computation of high-eccentricity orbits, by transforming time t to a new independent variable s. Once transformed, the integration in uniform steps of s effectively gives analytic step variation in t with larger time steps at apogee than at perigee, making errors at each point roughly comparable. In this paper, we develop techniques for assessing accuracy of s-integration in the presence of perturbations, and analyze the effectiveness of regularizing the transformed equations. A computational speed comparison is provided.

INTRODUCTION

Naval Space Command (NSC) has adopted a special perturbations catalog system, that is, orbit propagation based on a numerical integrator. It is more accurate than a general perturbations system which is based on analytic theory. The integrator forms a core routine in the parallel-processing space surveillance computation suite of programs known as SpecialK (Ref. 1). It is used for ephemeris generation and differential correction by both the automated parallel program and the manual maintenance program. This suite is used to maintain approximately 1300 satellites of greatest interest for space surveillance work; shortly, that number of satellites will grow to approximately 3300 and then the current catalog of 10,000 objects will be processed this way. Within the next ten years the NSC Service Life Extension Program will produce observations on 50,000 – 100,000 objects; these orbits will be maintained using special perturbations.

Because of the large number of satellites, attention must be paid to the total time of computation. For very eccentric orbits, satisfactory accuracy can be maintained with a larger step size near apogee than is used at perigee. One way to use a larger step at apogee is to make use of the known two-body orbit to transform the independent variable from time t to another variable s, $dt = cr^n ds$. This transformation, a generalized Sundman transformation (Ref. 2), allows one to use any numerical integration method in the independent variable s, which is thus called s-integration. Conventional time integration, by contrast, is called t-integration.

This paper presents a description of s-integration, including implementation, as well as a discussion and analysis of those orbits for which s-integration is preferable to t-integration. Since the goal of using s-integration is to save computation time, relative speed comparisons of s- versus t-integration are presented here. For orbits of sufficient eccentricity, the comparisons show a dramatic speedup over fixed-step t-integration, thus validating the original motivation for using s-integration.

*Graduate Assistant, Department of Aerospace and Ocean Engineering, Virginia Tech, Blacksburg, Virginia 24061, and Naval Research Laboratory, Code 8233, Washington, DC 20375-5355, E-mail: maberry2@vt.edu.

†Research Physicist, Naval Research Laboratory, Code 8233, Washington, DC 20375-5355, and Lecturer, Department of Aerospace Engineering, University of Maryland, College Park, MD 20742. E-mail: Liam.Healy@nrl.navy.mil.

We conclude with eccentricity values above which s-integration is advisable because there is a speed advantage without loss of accuracy.

GENERALIZED SUNDMAN TRANSFORMATIONS

Transformation equation

Sundman (Ref. 3) and Levi-Civita (Ref. 4), in attempting to solve the restricted problem of three bodies, introduced the transformation of the independent variable

$$dt = cr\,ds, \tag{1}$$

with c constant for the two-body orbit, because this transformation regularizes, and in fact linearizes, the equations of motion. Later investigators raised r to different powers in the transformation,

$$dt = cr^n\,ds, \tag{2}$$

known as the *generalized Sundman transformation* (Szebehely and Bond (Ref. 5) generalized even more, allowing an arbitrary function of r).

The new independent variable s is better understood in terms of an *orbit angle*. We give this term to any angle θ considered a function of true anomaly $\theta(\nu)$ that has the following properties:

- At perigee, the value of the angle is the same as true anomaly: $\theta(\nu) = \nu = 2\pi m$ for any integer m.
- At apogee, the value of the angle is the same as true anomaly: $\theta(\nu) = \nu = \pi m$ for any odd integer m.
- The angle increases monotonically with true anomaly, $\theta(\nu_2) > \theta(\nu_1)$ if $\nu_2 > \nu_1$.
- There is symmetry about the major axis: $\theta(\nu) = -\theta(-\nu)$.

Examples include the mean, eccentric, and true anomalies. Simply applying the transformation to s does not assure that s is then an orbit angle; c must be picked so that the appropriate boundary conditions are satisfied. The c necessary for the case $n = 3/2$ is computed in detail in the next section.

For each of the possible values of $n \geq 1$, there is a corresponding angle (Ref. 6, p. 100; Ref. 7; Ref. 8, p. 19; Ref. 9, p. 484):

- $n = 1$ or $dt = cr\,ds$. The angle s is the eccentric anomaly if c is chosen so that s is an orbit angle, $c = \sqrt{a/\mu}$. This case is Sundman's original transformation, or the Kustaanheimo-Stiefel transformation (Ref. 8).
- $n = 3/2$ or $dt = cr^{3/2}ds$. We shall focus on this transformation.
- $n = 2$ or $dt = cr^2ds$. The angle s is the true anomaly if c is chosen so that s is an orbit angle, $c = [\mu a(1 - e^2)]^{-1/2}$.

The constants c necessary for the cases of $n = 1$ and $n = 2$ can be derived from partial derivatives of the orbit angles. The partial derivative of the eccentric anomaly with respect to the mean anomaly is

$$\frac{\partial E}{\partial M} = \frac{a}{r}, \tag{3}$$

with a the semimajor axis. Because $M = mt$, where $m = \sqrt{\mu/a^3}$ is the mean motion, one may describe the differential relationship between time and eccentric anomaly E,

$$dt = \frac{1}{m}dM = \frac{r}{am}dE = r\sqrt{\frac{a}{\mu}}dE. \tag{4}$$

The relation between time and the true anomaly may be developed as follows. The partial derivative of true anomaly with respect to the mean anomaly is easy to compute,

$$\frac{\partial \nu}{\partial M} = \frac{a^2\sqrt{1-e^2}}{r^2} \tag{5}$$

where e is the eccentricity, M is the mean anomaly and ν is the true anomaly (Ref. 10). This relation gives us the time rate of change, since time is proportional to mean anomaly. Thus

$$dt = \frac{r^2}{\sqrt{a\mu(1-e^2)}} d\nu. \tag{6}$$

Ferrer and Sein-Echaluce (Ref. 11) showed that only $n = 1$ and $n = 2$ linearize the Kepler problem; the latter only with regularization. Palmer et al. (Ref. 12) studied the use of an $n = 1$ transformation for integration with a Bulirsch-Stoer integrator and compared results using positions obtained from a GPS-equipped satellite, but as described below, $n = 3/2$ is more commonly used for integration. Since perturbations affect the orbit, they also affect these transformations. However, the analysis that follows assumes a Kepler problem in order to understand the general characteristics of s-integration.

There are two ways we can approach a numerical integration implementation using these transformations. We can determine that the step size at perigee is fixed through the transformation; in this case, the total number of steps varies depending on the transformation. Expressing the transformations as orbit angles, Figure 1 illustrates this approach with an approximately fixed perigee step of $\Delta\nu \approx 1.0$ radian. Alternatively, one can fix the total number of steps on an orbit, and allow the step sizes to vary. Figure 2 illustrates this approach with sixteen points equally distributed in the same four orbit angles. The case of $n = 3/2$ represented as an orbit angle, called the intermediate anomaly, is discussed in the next section.

$n = 3/2$, or intermediate anomaly

Merson (Ref. 13) introduced the idea of using the value $n = 3/2$ in the generalized Sundman transformation, with an intent not of regularization *per se*, but of maximizing computational efficiency; see also Ref. 14. He gave an analysis showing that this value of n equally distributes the integration error around a full orbit, even if the eccentricity is high. One may conclude that this method is preferred for numerical integration. He also gave accuracy and timing results for $n = 3/2$, compared to other integrators. Nacozy (Ref. 7), like Merson, expressed s in terms of an elliptic integral of the true anomaly, and dubbed this angle the *intermediate anomaly*. His choice of constant $c = 1/\sqrt{\mu}$ made s dimensionless but does not result in an orbit angle; we show how to make s an orbit angle in this section.

For any exponent n, we may express the s differential element in terms of the true anomaly differential element using (6),

$$ds = \frac{1}{c} \frac{r^{2-n}}{\sqrt{\mu a(1-e^2)}} d\nu. \tag{7}$$

For $n = 3/2$, this relation simplifies to

$$ds = \frac{1}{c\sqrt{\mu}} \frac{d\nu}{\sqrt{1+e\cos\nu}}, \tag{8}$$

using the relationship $r = p/(1+e\cos\nu)$. Introducing the half angle $\theta = \nu/2$, the relation can be rewritten via a trigonometric identity

$$ds = \frac{1}{c\sqrt{\mu}} \frac{d\nu}{\sqrt{(1+e)\left(1-\frac{2e}{1+e}\sin^2\frac{\nu}{2}\right)}} = \frac{2}{c\sqrt{\mu(1+e)}} \frac{d\theta}{\sqrt{1-k^2\sin^2\theta}}, \tag{9}$$

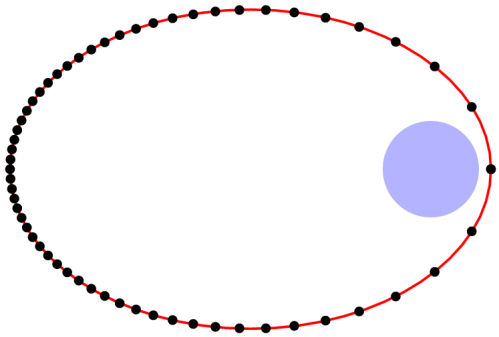

(a) Equal mean anomaly (n=0) with 58 steps.

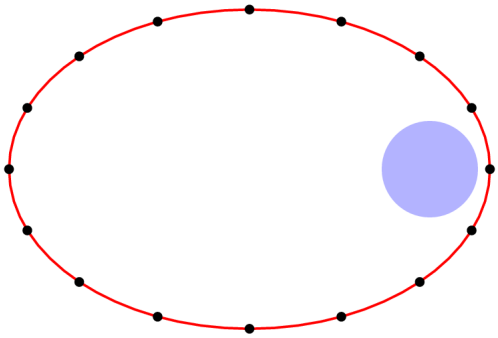

(b) Equal eccentric anomaly (n=1) with 16 steps.

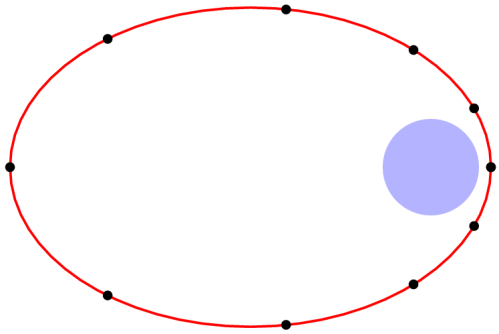

(c) Equal intermediate anomaly (n=3/2) with 10 steps.

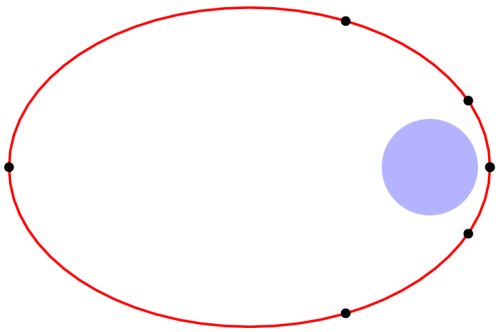

(d) Equal true anomaly (n=2) with 6 steps.

Figure 1: Points separated by equal values of various orbit angles, with the corresponding exponent n. Each orbit has approximately the same step size $\Delta\nu = 1$ radian at perigee.

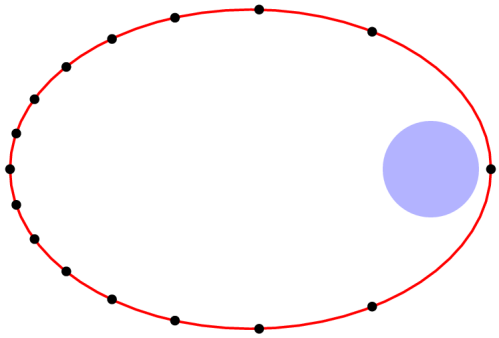

(a) Equal mean anomaly (n=0); step size at perigee is $\Delta\nu = 1.97$ radians.

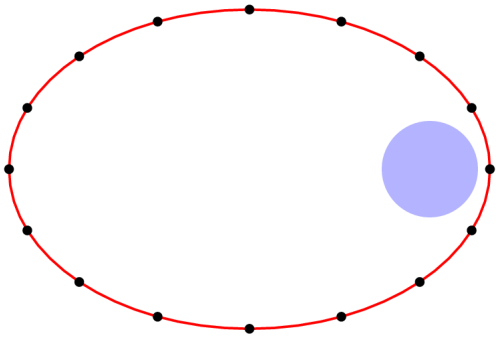

(b) Equal eccentric anomaly (n=1); step size at perigee is $\Delta\nu = 0.97$ radians.

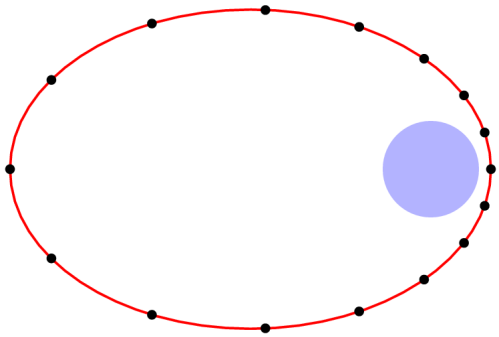

(c) Equal intermediate anomaly (n=3/2); step size at perigee is $\Delta\nu = 0.60$ radians.

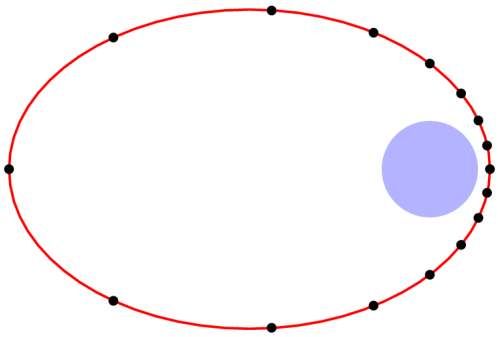

(d) Equal true anomaly (n=2); step size at perigee is $\Delta\nu = 0.39$ radians.

Figure 2: Points separated by equal values of various orbit angles, with the corresponding exponent n. There are 16 steps in each orbit.

where $k^2 = 2e/(1+e)$. Integrating (9), the second fraction is the incomplete elliptic integral of the first kind $F(\theta, k)$,

$$s = \frac{2}{c\sqrt{\mu(1+e)}} F\left(\frac{\nu}{2}, k\right). \tag{10}$$

In order to find c, we must match the boundary conditions. Evaluating (10) at perigee ($\nu = 0$), we have $s(0) = 0$ because $F(0, k) = 0$. Evaluating (10) at apogee, we require $s = \pi$ at $\nu = \pi$. Substituting the complete elliptic integral of the first kind $K(k)$ (Ref. 15, formula 17.3.2),

$$\pi = \frac{2}{c\sqrt{\mu(1+e)}} F\left(\frac{\pi}{2}, k\right) = \frac{2}{c\sqrt{\mu(1+e)}} K(k), \tag{11}$$

so

$$c = \frac{2K(k)}{\pi\sqrt{\mu(1+e)}}. \tag{12}$$

This value of c is what Merson (Ref. 13, p. 17) called an "augmentation factor." Outside of the half-plane between perigee and apogee, $0 \le \nu \le \pi$, the elliptic integral should be evaluated by making use of the elliptic integral magnitude recursion relation (Ref. 15, formula 17.4.3),

$$F(l\pi \pm \phi, m) = 2lK \pm F(\phi, m). \tag{13}$$

With $\bar{\nu} = \nu \mod 2\pi$, the change in true anomaly from the previous perigee passage, and $N = [\nu/2\pi]$, the number of whole orbits completed, s may be expressed as an orbit angle,

$$s = \begin{cases} 2\pi N + \dfrac{\pi}{K(k)} F\left(\dfrac{\bar{\nu}}{2}, k\right) & \text{if } 0 \le \bar{\nu} \le \pi, \\ 2\pi(N+1) - \dfrac{\pi}{K(k)} F\left(\dfrac{\bar{\nu}}{2}, k\right) & \text{if } \pi \le \bar{\nu} \le 2\pi. \end{cases} \tag{14}$$

This definition ensures symmetry about the major axis.

To solve for the true anomaly in terms of the intermediate anomaly, we must use the inverse of the elliptic integral, the Jacobian elliptic function. With

$$\frac{K(k)}{\pi} s = F\left(\frac{\nu}{2}, k\right), \tag{15}$$

we may write

$$\sin\frac{\nu}{2} = \operatorname{sn}\left(\frac{K(k)}{\pi} s\right), \tag{16}$$

and in the general case,

$$\nu = \begin{cases} 2\pi N + 2\arcsin\operatorname{sn}\left(\dfrac{K(k)}{\pi}\bar{s}\right) & \text{if } 0 \le \bar{s} \le \pi, \\ 2\pi(N+1) - 2\arcsin\operatorname{sn}\left(\dfrac{K(k)}{\pi}\bar{s}\right) & \text{if } \pi \le \bar{s} \le 2\pi, \end{cases} \tag{17}$$

where $\bar{s} = s \mod 2\pi$ and $N = [s/2\pi]$. These definitions complete the relationship between true anomaly ν and s as an orbit angle when $n = 3/2$. What follows in the rest of this paper does not depend on s being an orbit angle (that is, c can be any dimensionless number times $1/\sqrt{\mu}$).

Based on these formulas, it is straightforward to compute the ratio of the number of steps in a complete orbit for s-integration and t-integration when the two have the same step size at perigee (Fig. 1(a) and Fig. 1(c)). First, the constant step size in a given orbit angle is computed by converting the value in true anomaly at the first step after perigee to the orbit angle. Because all orbit angles are zero at perigee, this first step is the step size at perigee in the orbit angle. For the mean anomaly (t-integration) the conversion uses Kepler's equation; for the intermediate anomaly ($n = 3/2$ s-integration), we use (14). Since these step sizes are constant throughout the orbit for

the respective integration methods, the ratio of the number of points is the inverse of the ratio of the step sizes. This ratio is plotted as a function of eccentricity in Figure 3. For circular orbits ($e = 0$) the number of integration steps is exactly the same; as eccentricity increases, t-integration has proportionately more steps than s-integration. One might be tempted to conclude that it is never disadvantageous to use s-integration because it never has fewer integration steps if the perigee step size is chosen the same as t-integration. However this conclusion is not correct; additional computational costs are associated with s-integration in transforming the independent variable and integrating the transformation equation (2) that are not present for t-integration. Furthermore, perturbations affect the accuracy of s-integration more than that of t-integration, as we demonstrate in later sections.

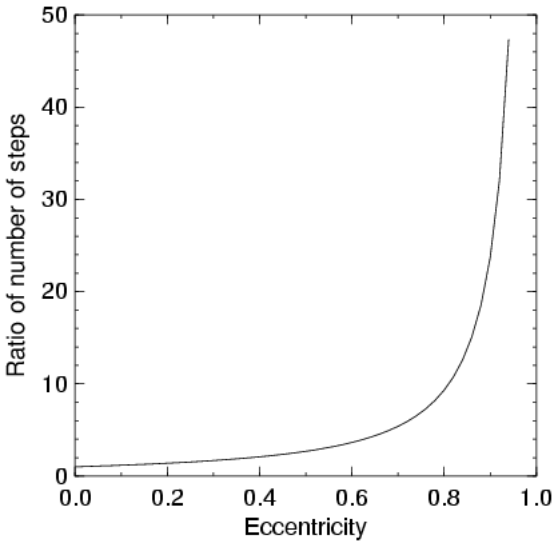

Figure 3: Ratio of the integration steps per orbit for t-integration to s-integration.

IMPLEMENTATION OF THE TRANSFORMATION

SpecialK has an eighth-order Gauss-Jackson integrator; it allows the user to choose either t-integration or s-integration. The s-integration is the Merson / Nacozy form discussed in the previous section with $n = 3/2$, but without regularization, and with $c = 1/\sqrt{\mu}$, so s is not an orbit angle. The implementation of t-integration is described in detail in (Ref. 16). Integration in s uses the same code, but adds the necessary transformation from t to s space; the transformation back into t space requires the integration of an additional, seventh, differential equation (2) to determine the time t.

The software first selects a step size in time. For s-integration the step size must be converted into s-space, and the conversion is performed using the distance from earth center to the satellite at perigee r_p,

$$\Delta s = \sqrt{\mu}\, r_p^{-\frac{3}{2}}\, \Delta t. \tag{18}$$

This makes the step at perigee the same in s-integration [Fig. 1(c)] as it is in t-integration [Fig. 1(a)].

After the step size is determined the integrator enters its initialization phase, which is necessary because the Gauss-Jackson method is a multi-step integrator. In the initialization phase the 8 positions and velocities surrounding epoch are first found using a fifth-order Taylor expansion of the two-body solution, known as the f and g series (Ref. 9) (Eq. 4-68). The t-integration initialization can be summarized:

Initialization for t-integration

1. Use f and g series to calculate 8 positions and velocities surrounding epoch.
2. Evaluate 9 accelerations from the positions and velocities, including epoch.
3. While the accelerations have not converged:
   (a) For each point $n = -4 \ldots 4, n \neq 0$:
      i. Calculate $\boldsymbol{r}_n$ and $\dot{\boldsymbol{r}}_n$, using Gauss-Jackson and summed Adams mid-corrector formulas.
      ii. Evaluate the acceleration $\ddot{\boldsymbol{r}}_n$ using the appropriate force model.
   (b) Test convergence of the accelerations.

A more complete description is available (Ref. 16, pp. 18-19).

Because the f and g series equations depend on the time between the points, and for s-integration the points must be equally spaced in s, a conversion must be made from s to time. To be exact, the time should be found by integrating (2); however, accuracy is not as critical in this first phase of the initialization routine, so the time is approximated by holding the epoch distance constant,

$$\Delta t_{fg} = \frac{r_0^{\frac{3}{2}}}{\sqrt{\mu}} \Delta s. \tag{19}$$

After the positions and velocities are calculated by the f and g series, the force model is evaluated to find the accelerations. These accelerations must then be converted to s-space by changing t derivatives to s derivatives.

The derivatives with respect to s are computed using the derivatives with respect to t via the relation

$$\frac{d}{dt} = c^{-1} r^{-n} \frac{d}{ds}. \tag{20}$$

Differentiation with respect to s will be indicated with a prime ($'$); that with respect to t by a dot ($\dot{}$). The velocity is converted by application of (20),

$$\dot{\boldsymbol{r}} = c^{-1} r^{-n} \boldsymbol{r}'. \tag{21}$$

The acceleration can then also be transformed,

$$\ddot{\boldsymbol{r}} = -c^{-3} c' r^{-2n} \boldsymbol{r}' - n c^{-2} r^{-2n-1} r' \boldsymbol{r}' + c^{-2} r^{-2n} \boldsymbol{r}'', \tag{22}$$

where $c' = dc/ds$ may be non-zero if perturbations are present (say, if c depends on a or e). In the present case $c = 1/\sqrt{\mu}$, and $n = 3/2$, so (22) can be solved for $\boldsymbol{r}''$,

$$\boldsymbol{r}'' = \frac{1}{\mu} \left(\frac{3}{2} r^2 \dot{r} \dot{\boldsymbol{r}} + r^3 \ddot{\boldsymbol{r}} \right). \tag{23}$$

This equation involves the derivative of the (scalar) magnitude r which is easily calculated,

$$\dot{r} = \frac{d\sqrt{\boldsymbol{r} \cdot \boldsymbol{r}}}{dt} = \frac{\boldsymbol{r} \cdot \dot{\boldsymbol{r}}}{r}, \tag{24}$$

so that the second derivative may be rewritten,

$$\boldsymbol{r}'' = \frac{1}{\mu} \left(\frac{3}{2} r (\boldsymbol{r} \cdot \dot{\boldsymbol{r}}) \dot{\boldsymbol{r}} + r^3 \ddot{\boldsymbol{r}} \right). \tag{25}$$

These second derivatives are then integrated using the Gauss-Jackson and summed Adams mid-corrector formulas to find the position and velocity at each of the 8 points surrounding epoch. The

integration does not give velocity directly; it gives $r' = dr/ds$. So a conversion must be made to find velocity,

$$\dot{\boldsymbol{r}} = \frac{\sqrt{\mu} r'}{r^{\frac{3}{2}}}. \tag{26}$$

Before the force model can be re-evaluated, the time at each point must be found. The time is found be integrating a seventh differential equation,

$$t' = \frac{1}{\sqrt{\mu}} r^{\frac{3}{2}}, \tag{27}$$

using the summed Adams mid-corrector formulas. With the time known the forces are evaluated to compute refined estimates of the accelerations, these accelerations are converted into s-space second derivatives, and the integration is performed again to obtain positions, velocities, and times at the points. This process repeats until the accelerations between two iterations converges to a prescribed tolerance. The initialization procedure for s integration may thus be summarized:
Inititalization for s-integration

1. Convert t step size to s step using the perigee distance, (18).
2. Use f and g series to calculate 8 positions and velocities surrounding epoch, holding the epoch distance constant to find the time, (19).
3. Evaluate 9 accelerations from the positions and velocities, including epoch.
4. Convert the accelerations into s derivatives, (25).
5. While the s second derivatives have not converged:
   (a) For each point $n = -4 \ldots 4, n \neq 0$:
      i. Calculate $\boldsymbol{r}_n$ and $\boldsymbol{r}'_n$, using Gauss-Jackson and summed Adams mid-corrector formulas.
      ii. Convert $\boldsymbol{r}'_n$ to $\dot{\boldsymbol{r}}_n$, (26).
      iii. Calculate the time at point n by integrating (27) with the summed Adams mid-corrector formulas.
      iv. Evaluate the acceleration $\ddot{\boldsymbol{r}}_n$ using the appropriate force model.
      v. Convert $\ddot{\boldsymbol{r}}_n$ to $\boldsymbol{r}''_n$, (25).
   (b) Test convergence of $\boldsymbol{r}''_n$.

After the integrator has completed the initialization process, it goes into a predictor-corrector cycle. In t-integration, the predictor formulas are first used to find the position and velocity at the next point, using the 9 known accelerations. The position and velocity are used to find the acceleration at that point, and that acceleration is then used in the corrector formulas to find more accurate values of the position and velocity. These values of position and velocity are then used to find a more accurate value of the acceleration and the corrector formulas are applied again. This process repeats until the position and velocity converge to a given tolerance. The predictor and corrector cycles for t-integration continue from steps 1-3 above as follows.
Predict (t-integration)

4. Calculate $\boldsymbol{r}_{n+1}$ and $\dot{\boldsymbol{r}}_{n+1}$, using Gauss-Jackson and summed Adams predictor formulas.

Evaluate — Correct (t-integration)

5. Evaluate the acceleration $\ddot{\boldsymbol{r}}_{n+1}$.
6. Increment n.

7. While $\boldsymbol{r}_n$ and $\dot{\boldsymbol{r}}_n$ have not converged:
   (a) Calculate $\boldsymbol{r}_n$ and $\dot{\boldsymbol{r}}_n$, using Gauss-Jackson and summed Adams corrector formulas.
   (b) Test convergence of $\boldsymbol{r}_n$ and $\dot{\boldsymbol{r}}_n$; if not converged, evaluate $\ddot{\boldsymbol{r}}_n$.
8. Predict next time step (go to 4).

This cycle is modified for s-integration. When the independent variable is s, the predictor (corrector) does not directly give velocity, it gives dr/ds, so the velocity must be found using (26). After the position and velocity are found the time at the new point must be found by solving (27) using the summed Adams predictor (or corrector) formula. After the forces are evaluated, the accelerations must be converted to second s derivatives using (25). Thus the predictor-corrector modified for s-integration continues from steps 1-5 above as follows:
Predict (s-integration)

6. Calculate $\boldsymbol{r}_{n+1}$ and $\boldsymbol{r}'_{n+1}$, using Gauss-Jackson and summed Adams predictor formulas.
7. Convert $\boldsymbol{r}'_{n+1}$ to $\dot{\boldsymbol{r}}_{n+1}$, (26).
8. Calculate the time at point $n+1$ by integrating (27) with the summed Adams predictor formula.

Evaluate — Correct (s-integration)

10. Evaluate the acceleration $\ddot{\boldsymbol{r}}_{n+1}$.
11. Convert $\ddot{\boldsymbol{r}}_{n+1}$ to $\boldsymbol{r}''_{n+1}$, (25).
12. Increment n.
13. While $\boldsymbol{r}_n$ and $\dot{\boldsymbol{r}}_n$ have not converged:
   (a) Calculate $\boldsymbol{r}_n$ and $\boldsymbol{r}'_n$, using Gauss-Jackson and summed Adams corrector formulas.
   (b) Convert $\boldsymbol{r}'_n$ to $\dot{\boldsymbol{r}}_n$, (26).
   (c) Calculate the time at point n by integrating (27) with the summed Adams corrector formula.
   (d) Test convergence of $\boldsymbol{r}_n$ and $\dot{\boldsymbol{r}}_n$; if not converged, evaluate $\ddot{\boldsymbol{r}}_n$, and convert to $\boldsymbol{r}''_n$.
14. Predict next time step (go to 6).

REGULARIZATION

The equations of motion contain the distance from the earth center to the satellite in the denominator, so a singularity exists; the equations are not regular. The equations can be regularized by introducing two-body conserved quantities (elements) that are redundant, such as the energy and the Laplace vector. These quantities must also be integrated if perturbations are present. Schumacher has suggested[1] that regularization should increase the accuracy of s-integration.

The equations may be regularized for any value of n and c with the following procedure (Schumacher, Ref. 2, pp. 17–24). The perturbed equation of motion,

$$\ddot{\boldsymbol{r}} + \frac{\mu}{r^3}\boldsymbol{r} = \boldsymbol{P}, \tag{28}$$

[1]Private communication.

where $\boldsymbol{P}$ is the perturbing acceleration, contains a singularity at $r = 0$ because of the reciprocal distance term. The acceleration $\ddot{\boldsymbol{r}}$ in (22) can be replaced using the equation of motion (28),

$$\boldsymbol{r}'' - nr^{-1}r'\boldsymbol{r}' + c^2\mu r^{2n-3}\boldsymbol{r} = c^2 r^{2n}\boldsymbol{P} + c^{-1}c'\boldsymbol{r}'. \tag{29}$$

In order to regularize this equation, the Keplerian energy, $\mathcal{E}$, and the Laplace vector, $\boldsymbol{B}$, must be introduced,

$$\mathcal{E} = \frac{1}{2}\dot{\boldsymbol{r}}\cdot\dot{\boldsymbol{r}} - \frac{\mu}{r}, \tag{30}$$

$$\boldsymbol{B} = \dot{\boldsymbol{r}}\times(\boldsymbol{r}\times\dot{\boldsymbol{r}}) - \frac{\mu}{r}\boldsymbol{r}. \tag{31}$$

These definitions can be transformed into s-space by using (21),

$$\mathcal{E} = \frac{1}{2}c^{-2}r^{-2n}(\boldsymbol{r}'\cdot\boldsymbol{r}') - \mu r^{-1}, \tag{32}$$

$$\boldsymbol{B} = c^{-2}r^{-2n}\boldsymbol{r}'\times(\boldsymbol{r}\times\boldsymbol{r}') - \mu r^{-1}\boldsymbol{r} \tag{33}$$

$$= c^{-2}r^{-2n}\boldsymbol{r}(\boldsymbol{r}'\cdot\boldsymbol{r}') - c^{-2}r^{-2n+1}r'\boldsymbol{r}' - \mu r^{-1}\boldsymbol{r}. \tag{34}$$

The first and third terms of the last equation resemble the terms in the energy equation, and the second term resembles the non-regular term in (29). So the energy and the Laplace vector can be combined to regularize (29),

$$nc^2r^{2n-2}(\boldsymbol{B} - 2\mathcal{E}\boldsymbol{r}) = -nr^{-1}r'\boldsymbol{r}' + c^2\mu r^{2n-3}\boldsymbol{r} + (n-1)c^2\mu r^{2n-3}\boldsymbol{r}; \tag{35}$$

notice that the $r^{2n-3}\boldsymbol{r}$ term has been deliberately split in two. Substituting the first two terms on the right side in $\boldsymbol{r}''$ equation (29) yields a regular equation,

$$\boldsymbol{r}'' - 2\mathcal{E}c^2nr^{2n-2}\boldsymbol{r} - (n-1)c^2\mu r^{2n-3}\boldsymbol{r} = -nc^2r^{2n-2}\boldsymbol{B} + c^2r^{2n}\boldsymbol{P} + c^{-1}c'\boldsymbol{r}', \tag{36}$$

which, because of the third term, is regular for $n = 1$ or $n \geq 3/2$. In the present case $n = 3/2$ and $c = 1/\sqrt{\mu}$, so (36) becomes

$$\boldsymbol{r}'' = \frac{3}{\mu}\mathcal{E}r\boldsymbol{r}' + \frac{1}{2}\boldsymbol{r} - \frac{3}{2\mu}r\boldsymbol{B} + \frac{1}{\mu}r^3\boldsymbol{P}, \tag{37}$$

which is the regularized equivalent of (25). When perturbations are present the time evolution of energy and the Laplace vector must also be determined by integration. To find the derivative of the energy first take a time derivative of (30),

$$\dot{\mathcal{E}} = \dot{\boldsymbol{r}}\cdot\ddot{\boldsymbol{r}} + \frac{\mu}{r^2}\dot{r}. \tag{38}$$

The right side of (38) is equivalent to taking a dot product of $\dot{\boldsymbol{r}}$ with the equation of motion (28), so

$$\dot{\mathcal{E}} = \boldsymbol{P}\cdot\dot{\boldsymbol{r}}. \tag{39}$$

Both sides can now be converted to s derivatives,

$$\mathcal{E}' = \boldsymbol{P}\cdot\boldsymbol{r}'. \tag{40}$$

By manipulating the equation of motion (28), the time derivative of the Laplace vector (31) can be shown to be

$$\dot{\boldsymbol{B}} = \boldsymbol{P}\times(\boldsymbol{r}\times\dot{\boldsymbol{r}}) + \boldsymbol{r}(\boldsymbol{r}\times\boldsymbol{P}) \tag{41}$$

$$= 2\boldsymbol{r}(\boldsymbol{P}\cdot\dot{\boldsymbol{r}}) - \dot{\boldsymbol{r}}(\boldsymbol{P}\cdot\boldsymbol{r}) - \boldsymbol{P}(\boldsymbol{r}\cdot\dot{\boldsymbol{r}}). \tag{42}$$

The time derivative can be converted to an s derivative,

$$\boldsymbol{B}' = 2\boldsymbol{r}(\boldsymbol{P}\cdot\boldsymbol{r}') - \boldsymbol{r}'(\boldsymbol{P}\cdot\boldsymbol{r}) - \boldsymbol{P}(\boldsymbol{r}\cdot\boldsymbol{r}'). \tag{43}$$

Regularization can be added to SpecialK in order to assess the effect on accuracy and computation speed. After the forces are evaluated, the two body acceleration is subtracted to give the perturbation acceleration, using (28). The perturbation acceleration is then used in (37) to give the second derivative, which is integrated numerically using the Gauss-Jackson method. The energy and the Laplace vector are also found by numerically integrating (40) and (43), respectively. These equations are integrated using the summed Adams method. Equations (30) and (31) are used to find the initial values of energy and the Laplace vector in the initialization routine. The procedure can be described as follows:
Initialization

1. Convert t step size to s step using the perigee distance, (18).
2. Find the initial energy and Laplace vector, (30) and (31).
3. Use f and g series to calculate 8 positions and velocities surrounding epoch, holding the epoch distance constant to find the time, (19).
4. Evaluate 9 accelerations from the positions and velocities, including epoch.
5. Calculate the perturbing acceleration from the total acceleration, (28).
6. Calculate the s derivatives, (37).
7. While the s second derivatives have not converged:
   (a) For each point $n = -4 \ldots 4, n \neq 0$:
      i. Calculate $\boldsymbol{r}_n$ and $\boldsymbol{r}'_n$, using Gauss-Jackson and summed Adams mid-corrector formulas.
      ii. Convert $\boldsymbol{r}'_n$ to $\dot{\boldsymbol{r}}_n$, (26).
      iii. Find the energy and Laplace vector at point n by integrating (40) and (43) with the summed Adams mid-corrector formulas.
      iv. Calculate the time at point n by integrating (27) with the summed Adams mid-corrector formulas.
      v. Evaluate the acceleration $\ddot{\boldsymbol{r}}_n$ using the appropriate force model, and find $\boldsymbol{P}$.
      vi. Calculate $\boldsymbol{r}''_n$, (37).
   (b) Test convergence of $\boldsymbol{r}''_n$.

Predict

8. Calculate $\boldsymbol{r}_{n+1}$ and $\boldsymbol{r}'_{n+1}$, using Gauss-Jackson and summed Adams predictor formulas.
9. Convert $\boldsymbol{r}'_{n+1}$ to $\dot{\boldsymbol{r}}_{n+1}$, (26).
10. Calculate the energy, Laplace vector, and time at point $n+1$ by integrating (40), (43), and (27) with the summed Adams predictor formula.

Evaluate — Correct

11. Evaluate the acceleration $\ddot{\boldsymbol{r}}_{n+1}$, and find $\boldsymbol{P}$.
12. Calculate $\boldsymbol{r}''_{n+1}$, (37).
13. Increment n.

14. While $\boldsymbol{r}_n$ and $\dot{\boldsymbol{r}}_n$ have not converged:

    (a) Calculate $\boldsymbol{r}_n$ and $\boldsymbol{r}'_n$, using Gauss-Jackson and summed Adams corrector formulas.

    (b) Convert $\boldsymbol{r}'_n$ to $\dot{\boldsymbol{r}}_n$, (26).

    (c) Calculate the energy, Laplace vector, and time at point n by integrating (40), (43), and (27) with the summed Adams corrector formula.

    (d) Test convergence of $\boldsymbol{r}_n$ and $\dot{\boldsymbol{r}}_n$; if not converged, evaluate $\ddot{\boldsymbol{r}}_n$, $\boldsymbol{P}$, and calculate $\boldsymbol{r}''_n$.

15. Predict next time step (go to 8).

COMPARISONS WITH t-INTEGRATION

A proposal to replace an existing t-integrator with an s-integrator for some or all orbits should weigh two considerations: the relative computation time and the relative accuracy. Two tests of t-integration and s-integration are considered in order to assess these factors:

- For testing without perturbations, the reference values are taken from the analytic two-body solutions.
- For testing with perturbations (24×24 WGS-84 geopotential, Jacchia 70 drag model, and lunar and solar perturbations), the reference values are taken by taking the final point of the integration and integrating backwards to epoch. This forward-backward test gives a rough indication of the integration error.

In all tests, a metric for integration accuracy is defined using an error ratio defined in terms of the RMS error of the integration (Ref. 13). First define position and velocity errors as

$$\Delta r = |r_{\text{computed}} - r_{\text{reference}}|, \tag{44}$$

$$\Delta v = |v_{\text{computed}} - v_{\text{reference}}|. \tag{45}$$

The RMS position error can be calculated,

$$\Delta r_{\text{RMS}} = \sqrt{\frac{1}{N}\sum_{i=1}^{N}(\Delta r_i)^2}, \tag{46}$$

with a similar equation for RMS velocity error. The RMS position error is normalized by the apogee distance and the number of orbits to find the position error ratio,

$$\rho_r = \frac{\Delta r_{\text{RMS}}}{r_A N_{\text{orbits}}}. \tag{47}$$

The velocity error ratio is found by normalizing by the perigee speed and the number or orbits,

$$\rho_v = \frac{\Delta v_{\text{RMS}}}{v_P N_{\text{orbits}}}. \tag{48}$$

Six orbits are considered, combinations of eccentricities of 0.0, 0.25, and 0.75 and perigee heights of 300 km, and 1000 km. All of the orbits have an inclination of 40°, and a ballistic coefficient of $0.01\,{}^{\text{m}^2}/_{\text{kg}}$. The epoch is 2001-10-01 00:00:00 UTC. Error ratios for position and velocity are found for each orbit with and without perturbations, using t-integration, s-integration, and s-integration with regularization. The error ratio for s-integration with perturbations using t-integration as the reference orbit is found with and without regularization. Each integration is for three days (72 hours), with a 30 second time step for t-integration, and the corresponding s step given by (18) for s-integration. The ephemeris is generated at one minute time intervals.

In cases where the step size used does not match the desired output points, SpecialK uses an interpolator. For these tests, the t-integration output points directly match the integration points, so no interpolation is needed. Interpolation is still needed, however, for s-integration, where the integration time does not occur at the step points. The interpolator normally used in SpecialK is a fifth-order interpolator for position, and a fourth-order interpolator for velocity; however, in order to get a fair comparison of t- and s-integration, an eighth-order Lagrange interpolator developed for these tests is used for the s-integration runs. This is the same order as the eighth order Gauss-Jackson integrator, and should insure no loss of accuracy during the s-integration runs.

Table 1 shows the results of the two-body test. Ephemeris is generated by SpecialK with all the perturbations turned off, and compared to the analytic solution. The ephemeris generated by t-integration is more accurate, most notably for the circular orbit. As the eccentricity is increased, the accuracy of s-integration approaches that of t-integration. Regularizing the s-integration does not show a significant improvement in accuracy.

Table 1: Error ratios for the two-body test relative to an analytic solution for t-integration, s-integration, and s-integration with regularization.

Test Case			Error Ratio		
e	h_p (km)		t	s	s-reg
0	300	pos	8.40×10^{-17}	8.94×10^{-12}	8.94×10^{-12}
		vel	8.40×10^{-17}	8.94×10^{-12}	8.94×10^{-12}
0	1000	pos	7.36×10^{-17}	4.33×10^{-11}	4.33×10^{-11}
		vel	7.36×10^{-17}	4.33×10^{-11}	4.33×10^{-11}
0.25	300	pos	8.05×10^{-16}	1.47×10^{-13}	1.40×10^{-13}
		vel	8.60×10^{-16}	1.57×10^{-13}	1.49×10^{-13}
0.25	1000	pos	8.25×10^{-17}	1.43×10^{-13}	1.45×10^{-13}
		vel	8.75×10^{-17}	1.52×10^{-13}	1.54×10^{-13}
0.75	300	pos	6.76×10^{-15}	1.55×10^{-14}	1.95×10^{-14}
		vel	1.25×10^{-14}	3.17×10^{-14}	3.73×10^{-14}
0.75	1000	pos	1.04×10^{-15}	1.14×10^{-13}	1.07×10^{-13}
		vel	2.27×10^{-15}	2.42×10^{-13}	2.27×10^{-13}

Table 2 shows the results of testing with perturbations. Each orbit is propagated forward 3 days with a 24×24 WGS-84 geopotential, Jacchia 70 drag model, and lunar and solar perturbations. The final value of the propagation is then used to propagate backwards to the original epoch. The error ratio shown is the difference between the forward and backward propagations. Again s-integration has a higher error ratio than t-integration, with a larger difference for the 1000 km orbits. In the presence of higher drag, t-integration and s-integration both lose accuracy and have closer error ratios. Again, s-integration with regularization has similar error ratios to s-integration without regularization, with some improvement showing at the higher eccentricity.

Table 3 shows the difference between the t-integration and s-integration forward propagations, as well as the difference between the t-integration and s-integration with regularization forward propagations. The higher perigee orbits have a closer agreement between t- and s-integration, which is consistent with the results from Table 2. Again the results for s-integration with and without regularization are similar.

A speed test is also performed for each orbit. The amount of time, in seconds, to propagate 30 days from epoch is shown for each integration type in Table 4. The test is performed on an SGI Origin 200, and the time shown is the user time. The 300 km circular orbit decays after 21 days, so the time shown is for a 20 day run. For the circular orbits, the t- and s-integration take the same amount of time, because there is no savings in integration steps for s-integration for a circular orbit. For the 0.25 eccentricity orbits there is a 1.5:1 time savings, and for the 0.75 eccentricity orbits there is a 6:1 savings. The s-integration with regularization has only a marginal cost in time over the

Table 2: Error ratios for test with perturbations, backward integration relative to forward.

Test Case			Error Ratio		
e	h_p (km)		t	s	s-reg
0	300	pos	4.93×10^{-9}	1.69×10^{-8}	1.69×10^{-8}
		vel	4.93×10^{-9}	1.69×10^{-8}	1.69×10^{-8}
0	1000	pos	3.38×10^{-12}	1.18×10^{-9}	1.18×10^{-9}
		vel	3.38×10^{-12}	1.19×10^{-9}	1.18×10^{-9}
0.25	300	pos	4.17×10^{-10}	9.38×10^{-9}	9.31×10^{-9}
		vel	4.44×10^{-10}	1.00×10^{-8}	9.93×10^{-9}
0.25	1000	pos	2.17×10^{-13}	2.72×10^{-10}	2.80×10^{-10}
		vel	2.32×10^{-13}	2.90×10^{-10}	2.99×10^{-10}
0.75	300	pos	5.78×10^{-9}	1.61×10^{-8}	1.56×10^{-8}
		vel	1.23×10^{-8}	3.38×10^{-8}	3.29×10^{-8}
0.75	1000	pos	3.61×10^{-12}	1.92×10^{-10}	1.18×10^{-10}
		vel	7.62×10^{-12}	4.07×10^{-10}	2.48×10^{-10}

Table 3: Error ratio of s-integration and s-integration using regularization with t-integration as the reference, with perturbations.

Test Case		Position Error Ratio		Velocity Error Ratio	
e	h_p (km)	s	s-reg	s	s-reg
0	300	1.24×10^{-8}	1.25×10^{-8}	1.24×10^{-8}	1.25×10^{-8}
0	1000	4.00×10^{-10}	4.00×10^{-10}	4.00×10^{-10}	4.00×10^{-10}
0.25	300	1.09×10^{-9}	1.14×10^{-9}	1.17×10^{-9}	1.22×10^{-9}
0.25	1000	9.19×10^{-11}	9.40×10^{-11}	9.74×10^{-11}	9.97×10^{-11}
0.75	300	4.42×10^{-8}	4.30×10^{-8}	9.41×10^{-8}	9.16×10^{-8}
0.75	1000	9.12×10^{-11}	4.46×10^{-11}	1.95×10^{-10}	9.22×10^{-11}

non-regularized s-integration.

Table 4: User time on an SGI Origin 200 to integrate 30 (*20*) days with perturbations.

Test Case		Time for 30 Day Run (sec)		
e	h_p (km)	t	s	s-reg
0	300	*21*	*21*	*22*
0	1000	31	31	32
0.25	300	29	20	21
0.25	1000	29	20	20
0.75	300	28	4.7	4.8
0.75	1000	28	4.6	4.7

The previous results show that when the step size for s-integration is chosen so that at perigee it uses the same step size as t-integration, s-integration is faster for integrating elliptical orbits but is not as accurate. This conclusion leads to another study, where the step size is chosen to give comparable accuracy between t-integration and s-integration. In this set of tests, the step size for each test case is found that gives an error ratio of approximately 1×10^{-9} in the forward-backward test. This step size is then used in a speed test, once again propagating 30 days forward from epoch with perturbations turned on. This test is performed to compare t-integration to s-integration without regularization; the previous results indicate that regularization does not yield a significant gain.

Table 5 shows the results for orbits with a 1000 km perigee height. Again, all of the test cases have an inclination of 40°, and a ballistic coefficient of $0.01\,{}^{\mathrm{m}^2}/_{\mathrm{kg}}$. The table shows the step size that gives an error ratio of 1×10^{-9} in the forward-backward test, and the time to propagate forward 30 days using that step size, for both t-integration and s-integration. The table also gives the ratio of the run-time for t-integration to the run-time for s-integration. When the ratio is greater than 1, s-integration is preferable. Table 5 shows that s-integration is preferable for $e \geq 0.15$. At eccentricities of 0.20 and 0.25, the step size used in s-integration is actually larger than the step size for t-integration, which indicates that for these step sizes s-integration is more accurate than t-integration. This is contrary to the results shown in Table 2, and this may mean that at the smaller step sizes used in Table 2, s-integration is affected by round-off error.

Table 5: User time on an SGI Origin 200 to integrate 30 days with perturbations, with the step size shown. Step size chosen to give an error ratio of 1×10^{-9}. Perigee height is 1000 km.

	Step Size		Time for 30 Day Run (sec)		
e	t	s	t	s	Ratio
0	50	30	18.3	31.0	0.59
0.05	55	54	16.7	16.4	1.0
0.10	64	58	14.2	14.0	1.0
0.15	73	72	12.2	10.3	1.2
0.20	70	74	12.6	9.17	1.4
0.25	68	80	12.8	7.80	1.6
0.50	61	61	14.0	5.80	2.4
0.75	65	51	13.1	2.94	4.5

The results for a perigee height of 300 km are shown in Table 6. In this case, s-integration is preferable for $e \geq 0.30$. The primary reason why these results differ from those of 1000 km is that the difference between the t-integration and s-integration step sizes needed to maintain a 1×10^{-9} error ratio is more significant. In the presence of higher drag, both t-integration and s-integration require a smaller step size than needed for the 1000 km case. However the step size has to be reduced more

dramatically for s-integration. Again this indicates that s-integration is being affected by round-off error more severely than t-integration. In fact, while searching for the step sizes needed for this test, we found that in some cases lowering the step size increased the error ratio. That may also be due to the nature of the forward-backward test, however. If s-integration is being affected by round-off error more severely than t-integration, the error is most likely coming from integrating the time equation, which is only needed in s-integration. More study is needed to determine if the error from integrating the time equation can be reduced.

Table 6: User time on an SGI Origin 200 to integrate 30 (*20*) days from epoch with perturbations, with the step size shown. Step size chosen to give an error ratio of 1×10^{-9}. Perigee height is 300 km.

	Step Size		Time for 30 Day Run (sec)		
e	t	s	t	s	Ratio
0	6	4	*99.6*	*153*	0.65
0.15	50	26	18.1	27.9	0.65
0.25	32	15	27.0	38.9	0.69
0.30	17	16	50.0	33.0	1.5
0.35	32	30	26.7	16.2	1.6
0.40	50	36	17.2	12.2	1.4
0.50	50	36	17.1	9.55	1.8
0.75	29	10	28.8	13.0	2.2

CONCLUSION AND FURTHER CONSIDERATION

It is possible to accelerate the numerical integration of orbits without loss of accuracy by transforming the independent variable from time (mean anomaly) to another variable s by the generalized Sundman transformation $dt = r^n ds$ for some exponent n. Existing literature indicates $n = 3/2$ is optimal for this purpose. For circular orbits, the two integration methods s and t have exactly the same number of points; for eccentric orbits, s-integration has fewer points on an orbit for equivalent accuracy. One might be tempted to conclude that s-integration is always indicated because it is never worse than t-integration. This is not so, however. A practical s-integration requires the integration of a seventh differential equation, the time equation, and also requires additional transformations to and from time. These have the effect of costing a small but measurable amount of computation time. Furthermore, the introduction of perturbations causes proportionately more inaccuracies than two-body motion because of the less-frequent force evaluation. For sufficiently low eccentricities, t-integration is faster for a given accuracy. A two-body analysis alone is not sufficient to determine, for a given orbit, which method is faster.

We sought to determine a threshold eccentricity above which s-integration is to be preferred because of decreased computation time for equivalent accuracy. It turns out this threshold is dependent on other orbit parameters, specifically, perigee height. Based on a study of the s and t integrators in the SpecialK code with step size set so that errors are comparable and a realistic set of perturbation forces, we have found that for a perigee height of 1000 km, the threshold is $e \approx 0.15$. At a lower perigee of 300 km, the threshold is $e \approx 0.30$. We believe the amount of drag the satellite experiences affects the round-off error and contributes to the determination of this threshold.

We found that regularization of the differential equations results in a minor improvement in accuracy for eccentricities higher than the threshold and does not justify the implementation or computation time.

Nacozy (Ref. 17) studied the time transformation equation (2) with the intent of finding alternate forms that may improve accuracy of the numerical integration of that equation. He suggested several reformulations of the time transformation equation that results in accuracy improvements of the

numerical integration of the time equation, including one that appears to be optimal for n=3/2. His test included only the two-body force and the J_2 perturbation on a satellite with $e = 0.3$, and no computation time cost is assessed. However, this work may be a fruitful area for further research in improving the s-integration results.

Another accuracy-related consideration that we have not addressed is stability in the Lyupanov sense: how much does a given small error in the orbital parameters contribute to error in the central angle, and thus to in-track position error, over a given period of time? Baumgarte (Ref. 18) discussed this problem and determined that the KS transformation ($n = 1$) improves orbit integration in this regard. This problem can be important because, while one integrator may have the same or even greater error ratio than another, it may still be more stable in the Lyapunov sense, and would keep the in-track errors more confined. Keeping the in-track errors confined increases the time span an orbit propagation remains accurate.

ACKNOWLEDGEMENTS

We thank Paul Schumacher for providing direction and insight into this problem. We thank Chris Hall, Fred Lutze, and Alan Segerman for helpful comments on the manuscript.

REFERENCES

[1] Neal, H. L., Coffey, S. L., and Knowles, S., "Maintaining the Space Object Catalog with Special Perturbations," In Hoots, F., Kaufman, B., Cefola, P., and Spencer, D., editors, *Astrodynamics 1997 Part II*, volume 97 of *Advances in the Astronautical Sciences*, pp. 1349–1360, San Diego, CA, August 1997. American Astronautical Society AAS 97–687.

[2] Schumacher, P. W., *Results of True-Anomaly Regularization in Orbital Mechanics*, PhD thesis, Virginia Polytechnic Institute and State University, Blacksburg, VA, 1987.

[3] Sundman, K. F., "Mémoire sur le Problème des trois corps," *Acta Mathematica*, Vol. 36, pp. 105–179, 1912.

[4] Levi-Civita, T., "Sur la résolution qualitative du problème restreint des trois corps," *Acta Mathematica*, Vol. 30, pp. 305–327, 1906.

[5] Szebehely, V. and Bond, V., "Transformations of the perturbed two-body problem to unperturbed harmonic oscillators," *Celestial Mechanics*, Vol. 30, No. 1, 1983, pp. 59–69, 1983.

[6] NORAD, *Mathematical Foundation for SCC Astrodynamic Theory*, Technical Report TP SCC 008, Headquarters North American Aerospace Defense Command, 1982. Obtainable from Defense Technical Information Center, Cameron Station, Alexandria, VA 22304-6145, as AD #B081394.

[7] Nacozy, P., "The intermediate anomaly," *Celestial Mechanics*, Vol. 16, pp. 309–313, 1977.

[8] Stiefel, E. L. and Sheifele, G., *Linear and Regular Celestial Mechanics*,, volume 174 of *Die Grundlehren der mathematischen Wissenshaften* Springer-Verlag, New York, 1971.

[9] Vallado, D. A., *Fundamentals of Astrodynamics and Applications*, McGraw-Hill, New York, 1997.

[10] Brouwer, D., "Solution of the problem of artificial satellite theory without drag," *Astron. J.*, Vol. 64, No. 1274, 1959, pp. 378–397, 1959.

[11] Ferrer, S. and Sein-Echaluce, M. K., "On the Szebehely-Bond equation. Generalized Sundman's transformation for the perturbed two-body problem," *Celestial Mechanics*, Vol. 32, No. 4, 1984, pp. 333–347, April 1984.

[12] Palmer, P. L., Aarseth, S. J., Mikkola, S., and Hashida, Y., "High precision integration methods for orbit propagation," *Journal of Astronautical Sciences*, Vol. 46, No. 4, 1998, pp. 329–342, October-December 1998.

[13] Merson, R. H., *Numerical Integration of the Differential Equations of Celestial Mechanics*, Technical Report TR 74184, Royal Aircraft Establishment, Farnborough, Hants, UK, January 1975. Defense Technical Information Center number AD B004645.

[14] Velez, C. E., "Notions of Analytic vs. Numerical Stability as Applied to the Numerical Calculation of Orbits," *Celestial Mechanics*, Vol. 10, pp. 405–422, 1974.

[15] Abramowitz, M. and Stegun, I. A., *Handbook of Mathematical Functions with Formulas, Graphs, and Mathematical Tables*,, volume 55 of *Applied Mathematics* National Bureau of Standards, Washington DC, 1964.

[16] Berry, M. and Healy, L., "Implementation of Gauss-Jackson Integration for Orbit Propagation," In *Advances in Astronautics*, San Diego, CA, August 2001. American Astronautical Society AAS 01–426; to appear.

[17] Nacozy, P., "Time elements in Keplerian orbital elements," *Celestial Mechanics*, Vol. 23, pp. 173–198, 1981.

[18] Baumgarte, J., "Numerical stabilization of the differential equations of Keplerian motion," *Celestial Mechanics*, Vol. 5, pp. 490–501, 1972.